The impact of hot-phonons on the performance of 1.3μm dilute nitride edge-emitting quantum well lasers

Roderick MacKenzie*[1]*, J. J. Lim[1], A.J. Kent[2], S. Sujecki[1] and E. C. Larkins[1]

[1] School of Electrical and Electronic Engineering
The University of Nottingham, University Park, Nottingham, NG7 2RD, U.K

[2] School of Physics and Astronomy
The University of Nottingham, University Park, Nottingham, NG7 2RD, U.K

The University of Nottingham

Accurate thermal modelling of optoelectronic devices

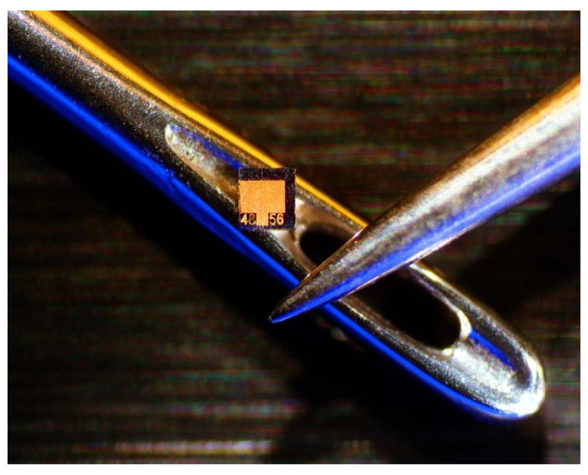

Figure 1. An example of a laser diode designed for use in severe environmental conditions such as on Mars

(Image courtesy of NASA)

- A state-of-the-art electro-optical-thermal device simulator to is extended to model
  - o Non-equilibrium LO-phonons generated via carrier relaxation in the QW
  - o Independent electron/hole temperatures
  - o Material gain dependent upon both electron and hole temperatures
- The impact of the non-equilibrium LO-phonon population on
  - o Optical and thermal transient response
  - o Light-current (LI) characteristics of the device are investigated
- Phonon bottle necks resulting in a LO-phonon temperature 7K higher than the lattice temperature were observed
  - o A corresponding reduction in optical power of up to 1mW was observed
- It was found particularly important to include hot phonon effects in dilute nitride devices due to the large conduction band offset

The Device

- Double quantum well GaInNAs laser diode
  - Optimised for uncooled 10Gb/s transmission at 1.3μm
  - Operates at heat sink temperatures of 110°C)
  - Low cost GaAs substrate
  - Good temperature stability $T_0 \approx$ 273K
  - 300μm cavity, uncoated facets and a ridge waveguide (RW) width of 3.2μm
  - Access market applications
- More details about this devices can be found elsewhere (Gustavsson *et. al.* 2006 *Electron. Lett.* **42** 925

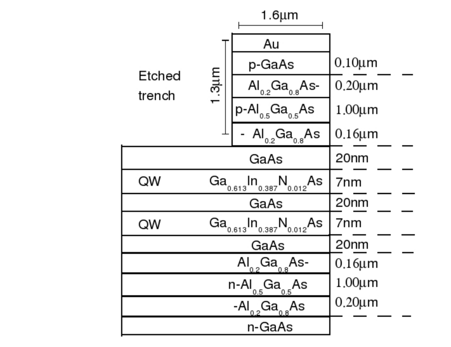

Figure 2. The epitaxy and structure of the device simulated

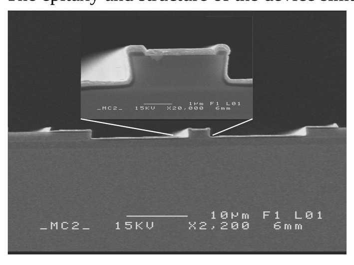

Figure 3. An SEM image of the ridge wave guide structure (Image courtesy of Chalmers University, Sweden)

The theoretical hot-phonon model

- Carrier are captured in to the QW from the bulk states heating the confined electron/hole populations. (Carriers also heated via Free Carrier Absorption)
  - Carrier gasses relax via dark recombination processes, LO-phonon, acoustic phonon and photon emission.
    - Carriers predominantly relax via the emission of LO-phonons
    - Due to the finite LO-phonon decay time an excess of LO-phonons can form around the QW
    - The hot-phonon population heats the carriers, thereby decreasing the optical gain
  - The non-equilibrium LO-phonon population relaxes to the lattice temperature via acoustic phonon emission.
- Heat propagates out of the device through the lattice
- Electrons/holes have independent quasi-Fermi levels and temperatures

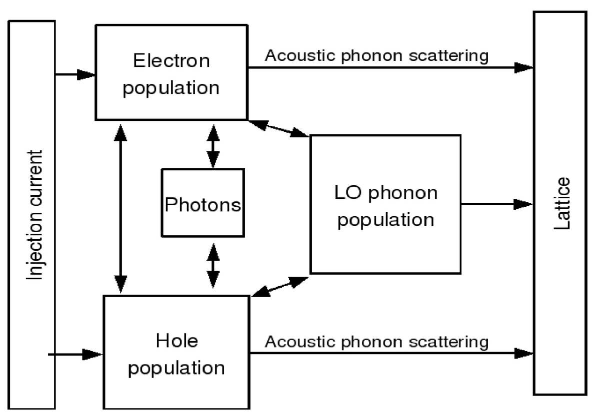

Figure 4. Schematic diagram of the energy pathways within the model.

The numerical model

The Electrical Model

- Bipolar 1D - 2D Drift Diffusion (DD) model (0th and 1st moments of the Boltzmann Transport Equation (BTE))
- Poisson's equation
- QW capture/escape equations for each QW
- 2D lattice heat equation solved in external solver

The Optical Model

- Photon rate equation for each QWs
- 2D mode solver
- Gain and spontaneous emission calculated using 4x4 band ***k.p*** solver

The Thermal Model

Lattice heat equation

$$C_L \frac{dT_L}{dt} = \nabla k_L \nabla T + H_{bulk} + \left(U^{LO}(T_{LO}) - U^{LO}(T_L)\right)/\tau_{LO-a} + \left(U^e(T_e) - U^e(T_L)\right)/\tau_{AC-e} + \left(U^h(T_h) - U^h(T_L)\right)/\tau_{AC-h}$$

Electron energy balance equation

$$\frac{dU_e}{dt} = H^e_{cap} + H^e_{SRH} + H^e_{Auger} + H^e_J - \overline{E}^{stim}_e R_{Stim} - \overline{E}^{spon}_e R_{Spon} - (U^e(T_e) - U^e(T_{LO}))/\tau_{LO-e} - (U^e(T_h) - U^e(T_L))/\tau_{AC-e} - (U^e(T_e) - U^e(T_h))/\tau_{e-h} + (U^h(T_h) - U^h(T_e))/\tau_{e-h}$$

Hole energy balance equation

$$\frac{dU_h}{dt} = H^h_{cap} + H^h_{SRH} + H^h_{Auger} + H^e_J - \overline{E}^{stim}_h R_{Stim} - \overline{E}^{spon}_h R_{Spon} - (U^h(T_h) - U^h(T_{LO}))/\tau_{LO-h} - (U^h(T_h) - U^h(T_L))/\tau_{AC-h} + (U^e(T_e) - U^e(T_h))/\tau_{e-h} - (U^h(T_h) - U^h(T_e))/\tau_{e-h}$$

LO-phonon energy balance equation

$$\frac{dU_{LO}}{dt} = (U^e(T_e) - U^e(T_{LO}))/\tau_{LO-e} + (U^h(T_h) - U^h(T_{LO}))/\tau_{LO-h} - (U^{LO}(T_{LO}) - U^{LO}(T_L))/\tau_{LO-a}$$

Carrier energy density

$$U_{e/h}(T) = \frac{\sum_N \int_0^\infty E D_{e/h}(E) f_{e/h}(E,T)\, dE}{L_w}$$

Average energy of lasing carriers

$$\overline{E}^{stim}_{e/h}(\hbar\omega) = \frac{\int_0^\infty \sum_N R^n_{stim}(\hbar\omega, E, T_e, T_h) L(\hbar\omega - E) E\, dE}{\int_0^\infty \sum_N R^n_{stim}(\hbar\omega, E, T_e, T_h) L(\hbar\omega - E)\, dE}$$

Average energy of spontaneous emission

$$\overline{E}^{spon}_{e/h} = \frac{\int_0^\infty \sum_N R_{Spon}(E_{eh}) E\, dE_{eh}}{\int_0^\infty \sum_N R_{Spon}(E_{eh})\, dE_{eh}}$$

LO-phonon energy density

$$U^{LO}(T) = \frac{\hbar\omega_{LO}}{(2\pi)^2} \int_{q^{min}_{xy}}^{q^{max}_{xy}} k_{xy} N(T)\, dk_{xy} \int_{-q_z}^{q_z} dq_z \quad \text{where,} \quad N(T) = \frac{1}{e^{\hbar\omega/kT} - 1}$$

This set of non-linear equations is solved using Newton's method.

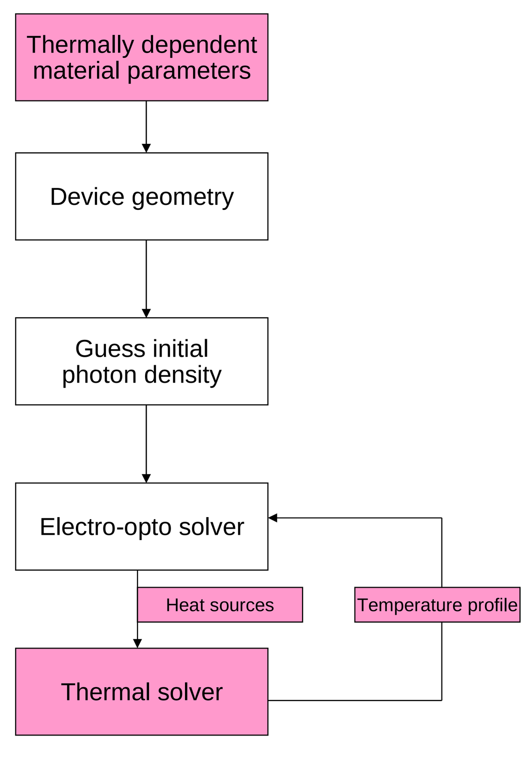

Figure 5. A flow diagram of the simulator used optimize the device

Definitions

Non-equilibrium LO phonon temperature	T_{LO}
Electron temperature	T_e
Hole temperature	T_h
lattice temperature	T_L
Capture heating	H_{CAP}
Free carrier absorption heating	H_{FCA}
Lateral joule heating	H_J
Stimulated emission rate	R_{Stim}
Spontaneous emission rate	R_{Spon}
Acoustic phonon relaxation time	$t_{AC-e/h}$
Carrier relaxation time	t_{LO-e}
LO phonon relaxation time	t_{LO-a}
QW carrier energy densities	$U_{e/h}$
Average lasing energy	E_{stim}
Average spontaneous emission energy	E_{spon}

Steady state results

Thermal profile

- A a typical simulated thermal profile of the device is shown in figure 6
- Free Carrier Absorption and Joule heating
  - Heat up the ridge
- The device can operate at heat sink temperatures up to 110°C

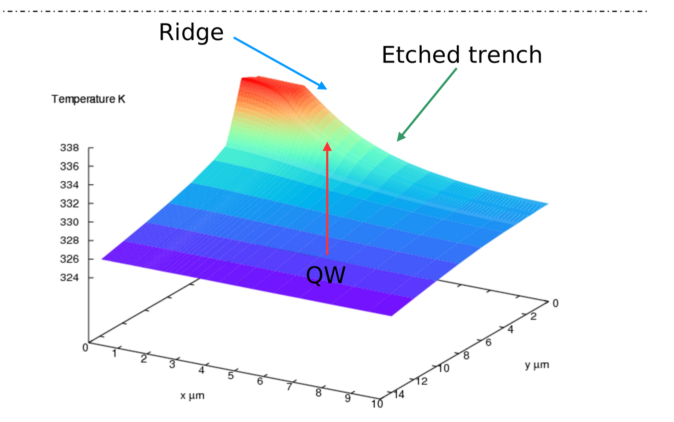

Figure 6. A typical device thermal profile, showing the ridge, etched trench and QW structure.

Hot carrier populations

- A thermal profile, corresponding to a front facet power of 12mW is plotted in figure 7, including electron, hole, non-equilibrium LO phonon and lattice temperatures.
- Under the ridge, the phonon bottleneck can be seen to elevate the carrier temperature by around 7K.
- The bottleneck corresponds to high carrier injection rates.
- Further away from the ridge, where the injection current is lower, the carrier/LO-phonon and lattice temperatures are the same.

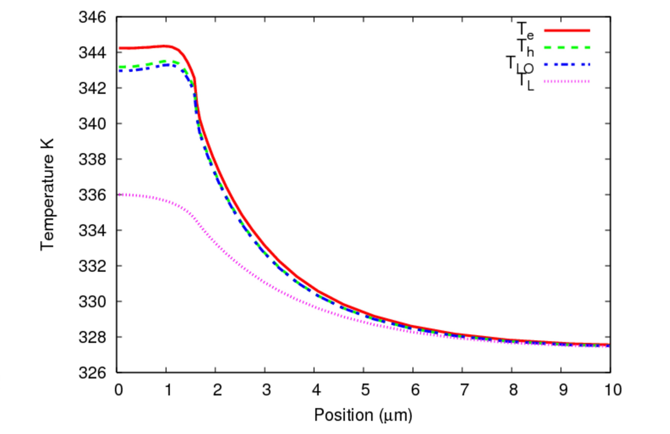

Figure 7, Cross section of the electron, hole, LO-phonon and lattice temperature with in the device.

Light-Current Characteristics

- A set of L-I curves for different phonon lifetimes is shown in figure 8.
- At high injection currents, the non-equilibrium LO-phonon temperature exceeds the lattice temperature by up to 15K
  - oThis causes a reduction of up to 1mW in optical power.
- At lower injection currents, a smaller impact on the L-I curve is observed.

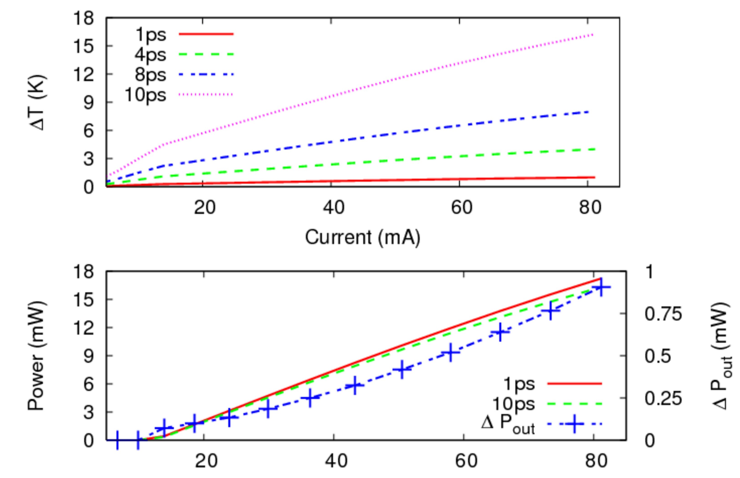

Figure 8, Front faces power verses injection current, Phonon bottle neck is also plotted.

Impact of heat sink temperature

- A super-linear increase in the LO-phonon temperature relative to the lattice temperature can be seen at heatsink temperatures above 360K.
- At lower heatsink temperatures (300-360K), the reduction in LO-phonon decay time as a function of temperature results in a very similar bottleneck for all temperatures.
- Experimentally, the device shows a decrease in performance for heatsink temperatures above 360K.
  - oThis could be partially attributed to the increasing impact of the LO-phonon bottleneck.

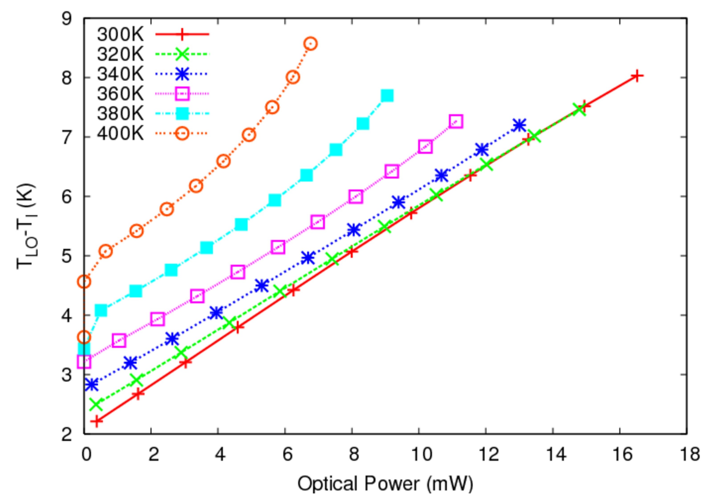

Figure 9, Phonon bottle neck as a function of Optical power for a range of heat sink temperatures.

Conclusion

- The phonon bottleneck is most important under the ridge, where the injection current is largest.
- At heatsink temperatures above 360K, the impact of the phonon bottleneck steadily increases.
- At high injection currents, the phonon bottleneck is seen to elevate the carrier temperature by up to 15K, with a corresponding decrease in optical power of up to 1mW.
- Modulation of the LO-phonon population is even observed under high speed modulation.

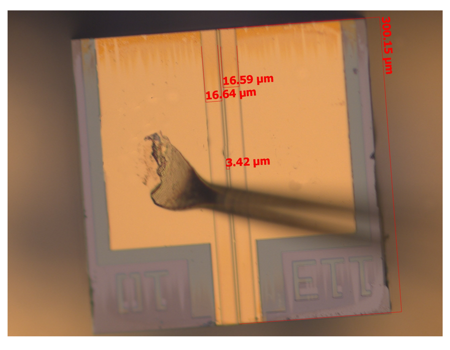

Figure 11. Optical image one of the device, the stripe of the ridge waveguide can be seen in the image

- The impact of hot phonons in dilute nitride devices is particularly large due to the large conduction band offset
- In order to accurately model the modulation response and thermal rollover in dilute nitride devices, hot phonon effects must be included in device models.

Time domain results

- A 1D time domain simulation at a bit rate of 10Gb/s is shown in figure 10.
- Inclusion of the non-equilibrium LO-phonon population
  - Elevates the carrier temperature with respect to the lattice temperature
  - Reduces the predicted peak optical power
  - Delays the peak of the optical pulse.
  - T_L=339K
- The non-equilibrium LO-phonon population increases its temperature by 3K within the width of the modulating pulse.

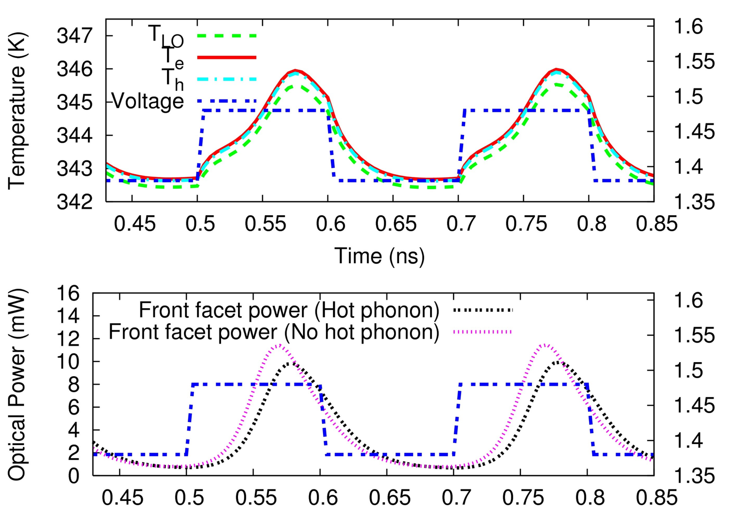

Figure 10, Time domain response to an input pulse

E-mail: eexrm1@nottingham.ac.uk

EPSRC Engineering and Physical Sciences Research Council

BRIGHT EU

FAST ACCESS

world-changing research from The University of Nottingham

The authors gratefully acknowledge the support of the EPSRC and the European Commission through the IST projects WWW.BRIGHT.EU and FAST ACCESS